

Modelling of the Nanowire CdS-CdTe Device Design for Enhanced Quantum Efficiency in Window Absorber Type Solar Cells

Kundan Kumar¹, Surendra Pattanaik², Dr. Saroj Kumar Dash³

^{1,2,3} Department of Electrical engineering,

Gandhi Institute of Technological Bhubaneswar Advancement (GITA), India

ABSTRACT

This paper presents Nano structuring is one of the most developed technologies that are able to improve considerably the photovoltaic conversion for low cost. This approach removes certain limitations of current technology; the photons that have low energy and do not participate in the photovoltaic conversion. Also, the photons that have a high energy that sell their excess energy in phonons' form. This work focuses on intermediate band solar cells introduced by material with a high-energy gap, an intermediate energy level, by quantum dots or quantum wells of some nanometers. This study attempts to show the great interest of this approach by calculating first, the efficiency limits of solar cell Shockley and interests in the intermediate-band photovoltaic solar cells approach by studying the parameters affecting their performances as well as the choice of materials and energy level of the nanostructure. All this, is achieved through the simulation software Matlab. The mathematical model developing stretches of photon emission by sun until the photovoltaic conversion in the semiconductor material

INTRODUCTION

Solar cells

The conventional energy sources like fossil fuels are going to deplete over the years and thus, the world is beginning to focus on renewable energy sources. The solar energy is abundant as well as environmentally friendly. It is versatile and the solar technology is making significant advances over the years. Since 2010, the world has added more solar photovoltaic (PV) capacity than in the previous four decades. The solar photovoltaic global capacity has been increased to 177 Gig watts in 2014, with an increase of 40 GW from 2013. [1] Figure1.1 shows the solarPV generation and projection until 2020 [2].

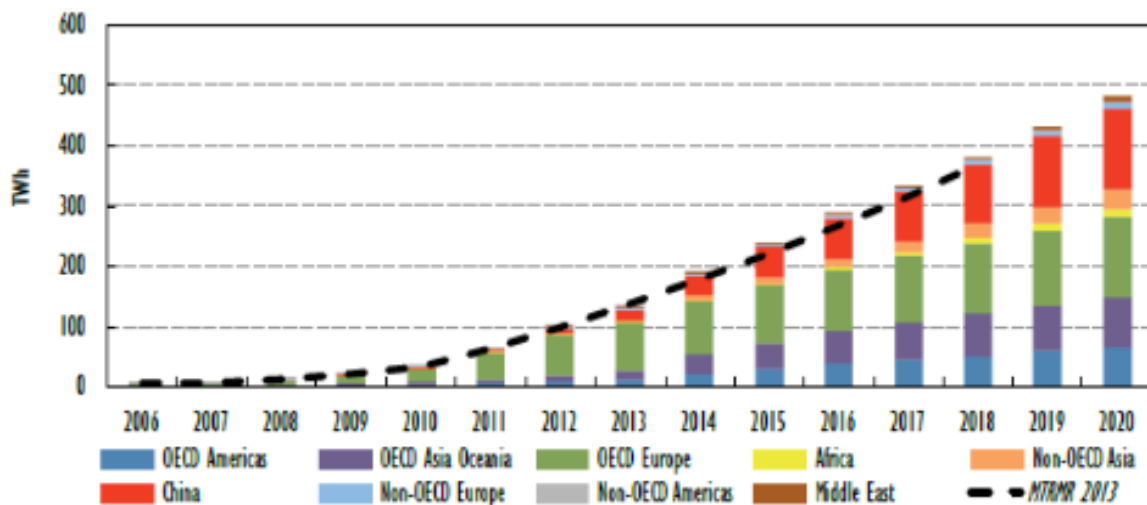


Figure 1.1 Solar PV generation and projection by region

Figure 1.2 shows the roadmap for PV's share of global electricity reaching 16% by 2050, a significant increase from the 11% goal in the 2010 roadmap [3].

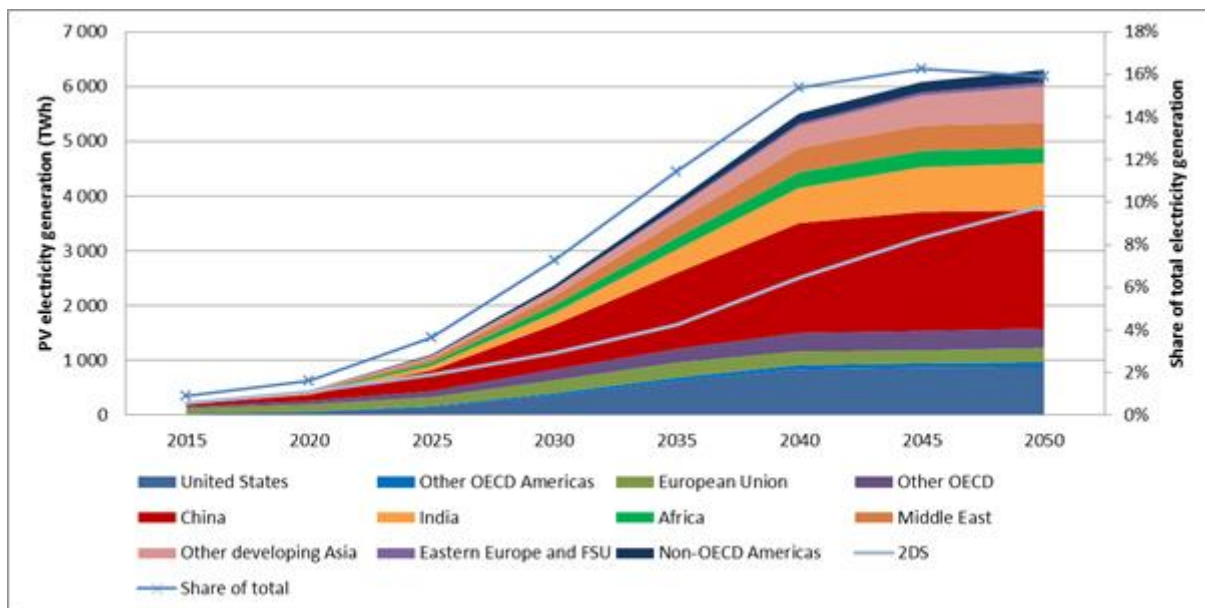


Figure 1.2 Regional production of PV electricity envisioned in the roadmap

The global investment in solar energy sector has increased by 25% in 2014 over 2013. Figure 1.3 shows the global new investment in Renewable energy [1].

History of solar cells

The photovoltaic effect was discovered by French physicist Alexandre-Edmond Becquerel in 1839. This was the beginning of the solar cell technology. In 1905, Albert Einstein published his paper on photoelectric effect that explained very well the absorption of the photons regarding to the frequency of light. Audobert and Stora discover the photovoltaic effect in cadmium sulfide (CdS) in 1932 [4]. Russell Ohl observed the first

photovoltaic effect of substantial EMF voltage on a silicon p-n junction in 1940 [5]. In 1954, Gerald Pearson, Daryl Chapin and Calvin Fuller, at Bell Laboratories discovered a silicon solar cell, which was the first material to directly convert sunlight into electricity to run electrical devices. The efficiency of this silicon solar cell, was 4%, which later increased to 11% [5]. Over several decades, different types of solar cells (multi-junction) using new materials have been fabricated in order to improve the efficiency of solar cells to reach Shockley – Queisser limit.

Generations of solar cells

Solar cells are mainly categorized into three generations. The first generation of solar cells has the major portion of the present market. The benefits of this solar cell technology are good performance and high stability. The materials use for this generation solar cells include GaAs and crystalline Silicon. However, the production costs is high due to high energy in production and material costs mostly for the silicon wafer. This generation of solar cells has higher efficiency (around 40%) as shown in Figure 1.4 [6]. The second generation of solar cells managed to reduce the material cost by eliminating the use of silicon wafer and replacing it with thin-film technology. This technology is based on amorphous silicon, CIGS, CdTe etc. where the typical efficiency is around 20% (Figure 1.4). The energy consumption associated with the production of these solar cells is quite high due to the use of vacuum processes and high temperature treatments. The third generation of solar cells includes Quantum Dot, Polymer, Perovskite, Nano crystalline and Dye- sensitized solar cells. The benefits of these types of solar cells are low cost and large scale production capability with flexibility. The disadvantages are low efficiency and low stability compared to traditional solar cells.

Quantum efficiency

Quantum efficiency is the ratio of the number of charge carriers collected by a solar cell to the number of photons of a given energy incident on the solar cell. It is related to the response of a solar cell to the various wavelengths in the spectrum of light which is incident on the cell. Thus, the quantum efficiency is expressed as a function of either wavelength or energy. There are two types of quantum efficiency of a solar cell. External quantum efficiency (EQE) considers the losses due to the recombination, transmission and reflection losses. It is the ratio of number of charge carriers collected by the solar cell to the number of incident photons of a given energy. Internal quantum efficiency (IQE) is the efficiency with which light not transmitted through or reflected away from the cell can generate charge carriers—specifically electrons and holes—that can generate current. By measuring the transmission and reflection of a solar device, the external QE curve can be corrected to obtain the internal QE curve. [7] Figure 1.6 [8] shows the curve of external quantum efficiency as a function of wavelength. The quantum efficiency is reduced by the surface recombination, reflection and low diffusion length. The quantum efficiency is also dependent on the series and shunt resistance, energy band gap and temperature.

Device Design

The device fabricated comprises of CdS nanowires which are embedded in a transparent anodized aluminum oxide (AAO) matrix. This device has been fabricated by Dr. Hongmei Dang for her PhD work [10]. The experimental procedures, figures 1.9-1.12 and the experimental results presented here are obtained from her dissertation. The schematic structure of the solar cell comprising of planar CdS and its carrier transport process is shown in figures 1.9 A and C respectively. Figure 1.9 B shows the structure of Nanowire CdS solar cell. Figure 1.9 D shows the carrier transport process of nanowire CdS/CdTe solar cell [10]. The use of AAO matrix and CdS nanowires in the nanowire CdS/CdTe solar cell resulted in the better transmittance of incident light, which improved the short circuit current. The open circuit voltage was improved due to the reduction of interface recombination and decreased effective reverse saturation current, which was the result of reduced junction interface area between the CdS nanowires and the polycrystalline CdTe.

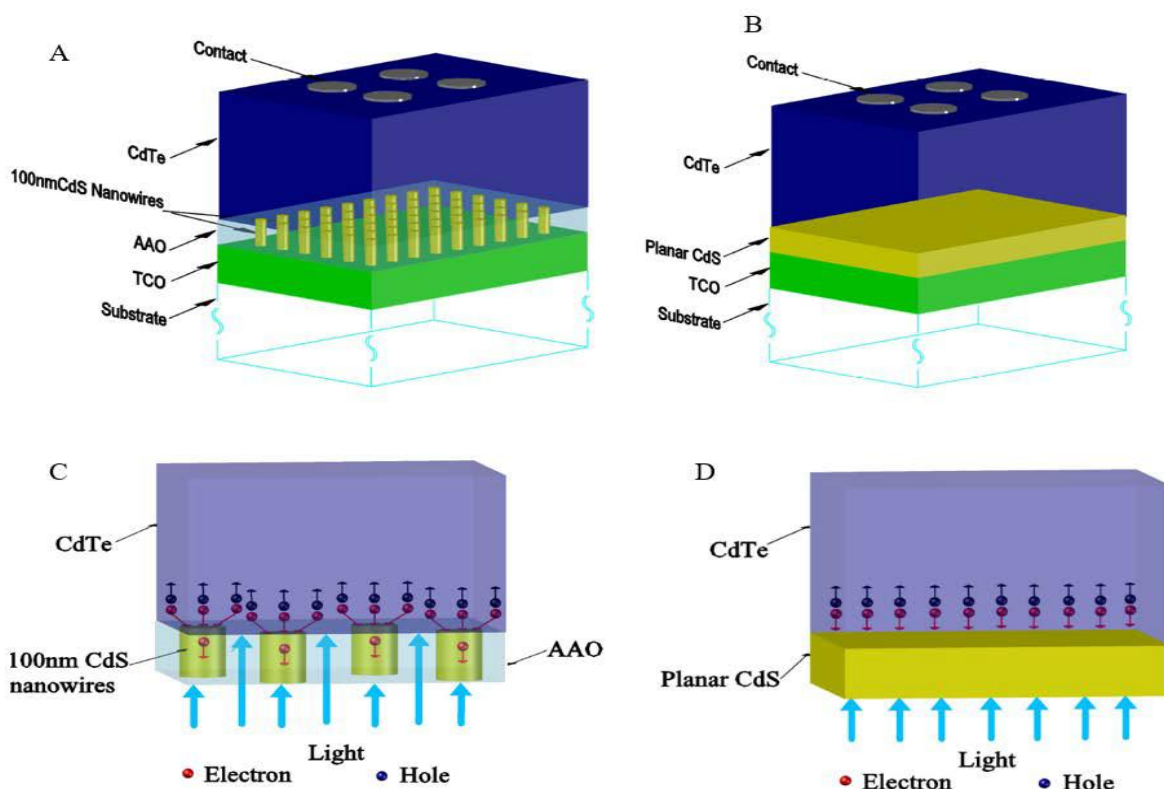


Figure 1.9 A. Schematic structure of a vertical stack nanowire CdS/CdTe solar cell, where light blue color represents absorption- negligible AAO, B. Schematic structure of a planar CdS/CdTe solar cell, C. Electron and hole transport through reduced junction interface area in a nanowire CdS/CdTe solar cell, D. Electron and hole transport through junction interface in a conventional planar CdS/CdTe solar cell [10]

Mathematical model of SCAPS-1D

Basic Equations

SCAPS-1D solves the one dimensional semiconductor equations. The equations areas follows:

A. Current –density equations:

The current conduction mainly consists of two components, namely drift component, which is caused by the electric field and diffusion component, which is caused by the carrier-concentration gradient. These are also called as the

Constitutive equations. [5]

The equations are as follows:

$$J_n = q\mu_n n \mathcal{E} + qD_n \frac{dn}{dx} = q\mu_n \left(n \mathcal{E} + \frac{kT}{q} \frac{dn}{dx} \right) = \mu_n n \frac{dE_{Fn}}{dx}$$

$$J_p = q\mu_p p \mathcal{E} + qD_p \frac{dp}{dx} = q\mu_p \left(p \mathcal{E} + \frac{kT}{q} \frac{dp}{dx} \right) = \mu_p p \frac{dE_{Fp}}{dx}$$

B. Continuity equations:

In semiconductor, there are various carrier transport mechanisms. The continuity equations include the time-dependent phenomena such as generation, recombination and low-level injection. The effect of drift, diffusion, indirect or direct thermal generation or recombination give rise to the change in carrier concentration with respect to time. The net change of carrier concentration is the difference between generation and recombination, plus the net current flowing in and out of the specified region.

The continuity equations are given by:

$$-\frac{\partial J_n}{\partial x} - U_n + G = \frac{\partial n}{\partial t}$$

$$-\frac{\partial J_p}{\partial x} - U_p + G = \frac{\partial p}{\partial t}$$

C. Poisson equation:

Poisson equation gives the starting point in obtaining the qualitative solution for electrostatic variables in a semiconductor. It is given by

$$\frac{\partial}{\partial x} \left(\epsilon_0 \epsilon \frac{\partial \Psi}{\partial x} \right) = -q(p - n + N_D - N_A)$$

Physical Model

For interface recombination, SCAPS-1D uses Pauwells Vanhoutte model [20]. The model considers four bands for interface states i.e. conduction and valence bands of both semiconductors at the interface.

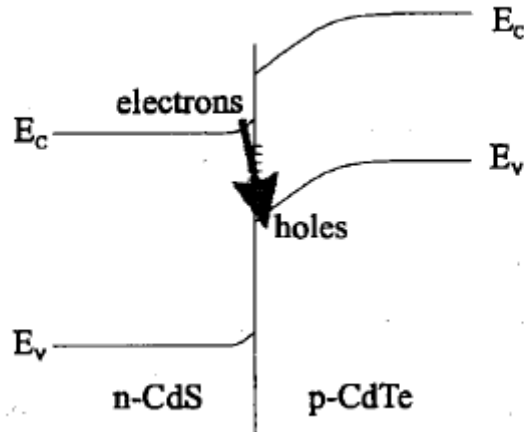


Figure 2.1 Pauwells Vanhoutte Model for CdS/CdTe heterojunction [20]

Crossover Effect

The crossover effect is generally observed in CdTe solar cells. At higher forward bias, the light current-voltage characteristic crosses over and reaches above the dark current-voltage characteristic. The crossover effect has been attributed to various causes including, (i) The photoconductivity effect; the bulk resistance of both CdS and CdTe is reduced when sunlight is shined on them. This leads to reduced series resistance and hence higher light current compared to the dark current is observed at voltages higher than the crossover point. (ii) Sensitivity of the CdS-CdTe heterojunction to the sunlight radiation; electron occupation of interface states and traps near the junction alters when sunlight falls on the device. This leads to a reduced junction potential barrier under illumination and hence higher light current compared to the dark current is observed at voltages higher than the crossover point. (iii) Sensitivity of the CdTe-Graphite Schottky diode junction to the sunlight radiation; some sunlight generated electrons reach the interface between the CdTe layer and the graphite electrode, and then recombine via surface states. This increases the value of the effective reverse saturation current (j_0) in light compared to the value of (j_0) in the dark, and leads to higher light current compared to the dark current at voltages higher than the crossover point. The simulations done by Burgelman et. al., in SCAPS-1D, have indicated that the crossover effect occurred due to the minority carrier recombination at metal/CdTe contact. [28] This recombination current is directly proportional to the illumination intensity. This needs to be added to the dark saturation current of the back diode. Thus, the total recombination current at illumination is higher than the dark, at a given voltage. It is negligible at low bias. However, it may become comparable with the back contact saturation current at higher bias. (iv) Sensitivity of the CdS/ i-SnO₂ junction to the sunlight radiation; some sunlight generated electrons reach the interface between the CdTe layer and i-SnO₂ layer, and then recombine via traps and interface states. This increases the value of the effective reverse saturation current (j_0) in light compared to the value of (j_0) in the dark, and leads to higher light current compared to the dark current at voltages higher than the crossover point. In our study, we focused on the fourth effect. The following curves

represent the J-V curves (dark and light) at 300K. Here, we see the crossover is starting to appear from Fig. 4.52 and crossover is observed at 0.96 V in fig. 4.53. Table 4.8 shows the parameters which were used for simulating these curves. The CdS thickness was reduced from 100 nm to 90 nm and the defect in i-SnO₂ layer was removed. We can conclude from here that the removal of defect in i-SnO₂ increases the J_{sc} at particular voltage, thus producing the crossover effect. Further, reducing the thickness of CdS layer reduced the overall resistance, thus increasing the current J_{sc}.

Rollover Effect

Because of the relatively high work function of p-CdTe, it is rather difficult to make an ohmic contact to it. To achieve a conducting contact, surface of CdTe must be cleaned, etched and its chemical composition modified in such a way that becomes tellurium rich, and highly conductive at the surface. In spite of careful processing, it is not uncommon for the CdTe-top electrode contact to become a Schottky diode. Many times, the solar cell, as made has a conducting contact between CdTe and the top electrode, but the contact degrades with time into a Schottky diode type because of insufficient encapsulation and the resultant oxidation of the CdTe surface. As this happens, the solar cell begins to behave like two back-to-back diodes [28-29]. One diode is made up of the main p-n heterojunction between n-CdS and p-CdTe, and the other is the Schottky diode between the surface of p-CdTe and the top electrode, which is typically graphite, or a metal like gold (Au). The current-voltage characteristics now display a saturation like behavior, which manifests as an S-shaped curvature in the I-V curve at high voltages. This effect, called the Rollover Effect, is illustrated in Fig. 4.54. It can be seen when the cell is the dark and also when under illumination. In the past, the Rollover Effect in planar CdS-CdTe solar cell devices has been explained by Singh et al [29] in terms of the tunneling breakdown of the Schottky diode; as thermionic emission and shunt conductance by Stollwerk et al [30]; and as drift and diffusion by Niemegeers et al [28]. Rollover effect can be explained by two diode model. The majority carrier current transport through CdTe back contact diode is limited by thermionic emission, or by drift and diffusion in the contact space charge layer, or a combination of both. However, slope of I-V curve at forward bias cannot be explained only by thermionic emission. The reason being current limited by thermionic emission is independent of voltage at forward bias. Further, the I-V curve shows a slope beyond the rollover point, which decreases exponentially with temperature. The shunt conductance at the contact, though shows the slope of I-V curve, does not explain the temperature dependence. According to Niemegeers et al [28], the current transport across the CdTe back contact is limited by drift and diffusion. The electric field at the metal contact depends on the voltage over the contact diode, which explains the voltage dependence of the saturation current. The Boltzmann factor $\exp(-q\phi_{BB})$ explains the temperature dependence of the saturation current. It is interesting to note that all of the three theories mentioned above, for the planar CdSCdTe solar cell device rely upon the presence of a diode at the junction between the surface of CdTe and the top electrode. To check the validity of these theories for the nanowire CdS-CdTe device, we simulated the effect of varying the height of the Schottky barrier on the current-voltage characteristics of the solar cell. The barrier height (energy difference between the metal Fermi level and

the top of the valence band) was altered from 0.5 eV to 0.4 eV. Fig. 4.54 shows the J-V curves (light) at 300 K shows parameters varied for removing the rollover effect. It is clear that the barrierheight of this Schottky diode at the CdTe surface plays a critical role in determining cell performance. The curve corresponding to the 0.5 eV barrier exhibits a strong rollover effect, while this effect has disappeared when the barrier was reduced to 0.4 eV. The fact that the 2-diode model is applicable to the nanowire CdS-CdTe-graphite solar cell as the planar CdS-CdTe-graphite cell is not surprising because the CdTe-graphite junction is the same in both cases.

Simulation

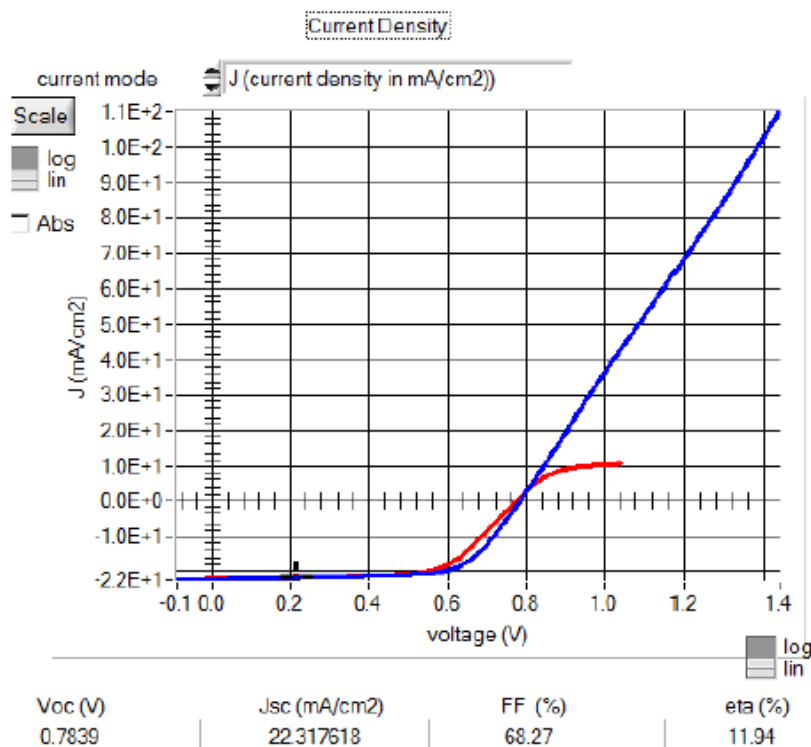


Figure 4.54 Simulated J-V curves (light) at 300 K

	Red curve	Blue Curve
Majority carrier barrier height [relative to E_f](eV)	0.5	0.4
Majority carrier barrier height [relative to E_v](eV)	0.3271	0.2271

Parameters varied for removing the rollover effect

Conclusion and Future Work

CdS nanowires have several advantages over the planar CdS such as the improvement in open circuit voltage due to reduced junction area and improvement in short circuit current due to higher optical transmission through CdS nanowires. The modeling of the nw-CdS/ CdTe was studied by using SCAPS-1D in order to identify and evaluate the parameters responsible for improving the efficiency of this solar cell. The effects of various parameters including interface state density, CdS and CdTe state densities, trap concentration, metal work function on light I-V curves were studied and the optimum values for these parameters were obtained in order to get the highest efficiency without convergence failure and with no crossover or rollover effect. The highest efficiency for nw-CdS/ CdTe structure obtained was 22.26% with $J_{sc} = 26.724 \text{ mA/cm}^2$, $V_{oc} = 0.9828 \text{ V}$ and $FF = 84.27$ at 300K. It can be concluded here that the efficiency can be improved by improving the interface and contact properties of nw CdS/CdTe structure. The fill factor can be improved by reducing the series resistance and increasing the shunt resistance. The simulations for J-V characteristics of nw-CdS/CdTe solar cell were performed using SCAPS-1D for getting the curve fit with the experimental characteristics for 300 K. The experimental J-V measurements at 300 K were $V_{oc} = 0.770 \text{ V}$, $J_{sc} = 26 \text{ mA/cm}^2$, $FF = 60\%$ and the efficiency of 12%. The simulated J-V curves considered for curve fitting were at $V_{oc} = 0.7919 \text{ V}$, $J_{sc} = 22.345 \text{ mA/cm}^2$, $FF = 68.27\%$ for the efficiency of 12.08%. The same parameters were used for obtaining the simulated J-V characteristics at lower temperatures 275K, 250K and 225K. It can be concluded here that the simulated J-V characteristics were close to the experimental characteristics with $R^2 > 0.9$ at all temperatures. The variations in V_{oc} and J_{sc} can be attributed to the defects, assumptions made in the simulations for nw-CdS parameters and SCAPS-1D does not consider parameters such as energy bandgap and mobilities as temperature dependent. Further, it was observed that the present simulated model explains the important effects of the nw-CdS/CdTe solar cell such as crossover and rollover effect. The crossover effect was studied by considering the sensitivity of CdTe/i-SnO₂ under illumination. It was shown that the removal of defect in i-SnO₂ is responsible for producing the crossover effect. The rollover effect has been explained by using back to back diode model in the literature and the simulations were performed in order to validate this theory. It was shown that the change of barrier height at the contact is a critical parameter in the rollover effect. Once the majority carrier barrier height was varied from 0.4 to 0.5 eV, the curve corresponding to the 0.5 eV barrier showed a strong rollover effect, while this effect was disappeared when the barrier was reduced to 0.4 eV. Overall, it can be concluded that SCAPS-1D model, which is modeled for thin film solar cells, is able to provide the realistic simulation for nw-CdS/CdTe solar cells. For future work, C-V and external quantum efficiency (EQE) characteristics can be simulated, studied and the results can be compared with the experimental obtained data.

References

- [1] Renewable Energy Policy Network for the 21st Century (Ren21), "Renewables 2015 Global status report". Available from: <http://www.ren21.net/status-of-renewables/globalstatus-report/> (2015)
- [2] Agency, I.E., Medium-Term Renewable Energy Market Report 2014, Paris (2014)

- [3] Agency, I.E., Technology Roadmap: Solar Photovoltaic Energy (2014)
- [4] Vesselinka Petrova-Koch, Rudolf Hezel, Adolf Goetzberger, "High -Efficient Low-Cost Photovoltaics: recent Developments", Springer series in optical sciences (2008)
- [5] S.M. Sze, K. K. N., "Physics of semiconductor devices" (2007)
- [6] Laboratory, N. R. E., "solar cell efficiency chart", Available from:<http://www.nrel.gov.ncpv> (2015)
- [7] Department, E., <http://energy.gov/eere/energybasics/articles/photovoltaic-cellquantum-> efficiency-basics (2016).
- [8] Photovoltaic Education Network, <http://pveducation.org/pvcdrom/solar-celloperation/quantum-efficiency> (2016)
- [9] Purnomo Sidi Priambodo, Didik Sukoco, Wahyudi Purnomo, Harry Sudiby and Djoko Hartanto (2013). Electric Energy Management and Engineering in Solar Cell System, Solar Cells - Research and Application Perspectives, Prof. Arturo Morales- Acevedo (Ed.), ISBN: 978-953-51-1003-3, InTech, DOI: 10.5772/52572. Available from: <http://www.intechopen.com/books/solar-cells-research-and-applicationperspectives/electric-energy-management-and-engineering-in-solar-cell-system>
- [10] Hongmei Dang, "Nanostructured Semiconductor Device Design in Solar Cells", Ph.D. Thesis, University of Kentucky (2015). Available from: http://uknowledge.uky.edu/ece_etds/77/
- [11] Marc Burgelman, Johan Verschraegen, Stefaan Degraeve and Peter Nollet," Modeling Thin-film PV Devices", Progress in Photovoltaics: Research and Applications, , 143–153 (2004)
- [12] M. S. Lundstrom, "Numerical Analysis of Silicon Solar cells" (1980)
- [13] J. L. Gray, "A computer model for the simulation of thin-film silicon-hydrogenalloy solar cells," IEEE Transactions on Electron Devices, 36, 906-912 (1989)
- [14] E. K. Banghart, "Physical mechanisms contributing to nonlinear responsivity in silicon concentrator solar cells" (1989).
- [15] P. D. DeMoulin and M. S. Lundstrom, "Projections of GaAs solar-cell performance limits based on two-dimensional numerical simulation," IEEE Transactions on Electron Devices, 36, 897-905 (1989).
- [16] Analysis of Microelectronic and Photonic Structures (AMPS) software, developed at Pennsylvania State University. Also, see <http://www.psu.edu/dept/AMPS>
- [17] Schropp R, Zeman M., "Amorphous and Microcrystalline Silicon Solar Cells"Kluwer: Boston, (1998).